Journal of The Electrochemical Society, **147** (9) 3420-3428 (2000)
S0013-4651(99)12-021-4 CCC: $7.00

Elucidation of the Mechanism of Dioxygen Reduction on Metal-Free Carbon Electrodes

Hsueh-Hui Yang and Richard L. McCreery*,z

Department of Chemistry, Ohio State University, Columbus, Ohio 43210-1185, USA

On a glassy carbon (GC) surface covered with a covalently bonded methylphenyl monolayer, O_2 reduction to superoxide was observed and shown to be chemically reversible above pH 10. The voltammetry is completely explained by electron tunneling through the organic monolayer, then degradation of $O_2^{\bullet -}$ in aqueous solution by known homogeneous mechanisms. As the pH is decreased below about 10, $O_2^{\bullet -}$ in solution decays to O_2 and H_2O_2 by routes previously deduced from pulse radiolysis experiments. In contrast, a GC surface cleaned with isopropanol and activated carbon is very active toward adsorption, and a two electron reduction to peroxide is observed. An adsorbed intermediate is proposed to be a surface hydroperoxide analogous to stable organic peroxides of the general formula ROOH. On clean, unmodified GC, the pH dependence of the O_2 reduction mechanism is consistent with control of the reduction process by adsorbed $O_2^{\bullet -}$ or $^{\bullet}O_2H$. In the absence of adsorption sites on the carbon surface, degradation of electrogenerated superoxide occurs entirely in solution.

Manuscript submitted December 6, 1999; revised manuscript received April 22, 2000.

The oxygen reduction reaction has been studied extensively on metal electrodes (Pt, Hg, Ag, and Au) and nonmetal electrodes (carbon, diamond, and metal oxides), due mainly to the importance of dioxygen reduction to electrochemical energy conversion.[1-18] Many different types of carbon have been studied, such as highly ordered pyrolytic graphite (HOPG), pyrolytic graphite (PG), graphite powder, porous graphite, natural graphite, glassy carbon (GC), pyrolytic carbon, active carbon, carbon black, and carbon single crystals. The effect of electrode material on the O_2 reduction reaction (ORR) has been reviewed extensively,[1-3] but detailed mechanisms remain elusive. On metal electrodes, O_2 reduces by either $2e^-$ to H_2O_2, or $4e^-$ to H_2O, depending on the electrode material and surface modifications. The ORR on metals is often controlled by chemisorption of O_2 or its reduction products, particularly metal oxides, superoxide, and hydrogen peroxide, and by chemisorbed anions.[1,2] On carbon surfaces, the reduction product is H_2O_2 or HO_2^-, depending on pH, and the electrode kinetics are much slower than those on active metals such as platinum and gold. Various catalysts have been used to modify carbon electrodes to promote the disproportionation of H_2O_2 or to effect a $4e^-$ reduction[7,8,19-26] by either the peroxide pathway or direct $4e^-$ reduction on a modified carbon surface. A practically important example is the reduction of O_2 in alkaline media with a carbon surface modified with metal phthalocyanines, used in zinc/air batteries and the air cathode. While carbon surfaces modified with metal-containing catalysts have resulted in elegant chemistry and important applications, they are not the subject of the current investigation. We focus here on the mechanism of the ORR on carbon in the absence of metal catalysts.

An overview of the literature on the ORR on carbon surfaces reveals that there is no consensus on the mechanism or even the identity of adsorbed intermediates. Most researchers conclude that the adsorption of O_2 or superoxide is involved, but variations in surface conditions and pretreatment cause wide variations in electrode behavior. Consequently, there is substantial disagreement among ORR mechanisms proposed in the literature. For example, Taylor and Humffray[16] concluded the following mechanism for GC electrodes

$$O_2 + e^- \rightleftarrows O_{2(\text{ads, before migration})}^{\bullet -} \quad [1]$$

$$O_{2(\text{ads, before migration})}^{\bullet -} \rightleftarrows O_{2(\text{ads, after migration})}^{\bullet -} \quad [2]$$

$$2\, O_{2(\text{ads, after migration})}^{\bullet -} + H_2O \rightleftarrows O_2 + HO_2^- + OH^- \quad [3]$$

Surface migration of adsorbed O_2^- (reaction 2) to the active sites was proposed to be the rate-determining step. Zhang *et al.*[17] proposed two different forms of adsorbed O_2 on a GC surface, with Reaction 6 suggested as the rate-determining step

$$O_2 + e^- \rightleftarrows [O_{2(ads)}]^{\bullet -} \quad [4]$$

$$[O_{2(ads)}]^{\bullet -} \rightleftarrows \{O_{2(ads)}\}^{\bullet -} \quad [5]$$

$$\{O_{2(ads)}\}^{\bullet -} + H_2O \rightleftarrows HO_{2(ads)}^{\bullet} + OH^- \quad [6]$$

$$HO^{\bullet}_{2(ads)} + e^- \rightleftarrows HO^-_{2(ads)} \quad [7]$$

$$HO^-_{2(ads)} \rightleftarrows HO_2^- \quad [8]$$

$[O_{2(ads)}]^{\bullet -}$ and $\{O_{2(ads)}\}^{\bullet -}$ represent two different forms of superoxide on the surface, with and without an O-O bond. Appleby and Marie[5] proposed a mechanism involving a second electron transfer on carbon black electrodes in alkaline solution

$$O_2 + e^- \rightleftarrows O_2^{\bullet -} \quad [9]$$

$$O_2^{\bullet -} + H_2O + e^- \rightleftarrows HO_2^- + OH^- \quad [10]$$

or

$$O_2 + H_2O + e^- \rightleftarrows HO_{2(ads)}^{\bullet} + OH^- \quad [11]$$

$$HO_{2(ads)}^{\bullet} + e^- \rightleftarrows HO_2^- \quad [12]$$

where Reaction 10 or Reaction 12 is the rate-determining step.

More recently, Xu *et al.*[12] explored several different carbon surfaces, including electrochemically pretreated GC, laser-treated GC, fractured GC, low defect HOPG basal plane surfaces, and modified GC. They proposed the following mechanism

$$O_2 + e^- \rightleftarrows O_{2(ads)}^{\bullet -} \quad [13]$$

$$O_{2(ads)}^{\bullet -} + H_2O \rightleftarrows HO_{2(ads)}^{\bullet} + OH^- \quad [14]$$

$$HO_2^{\bullet} + O_2^{\bullet -} \rightleftarrows HO_2^- + O_2 \quad [15]$$

or

$$HO_{2(ads)}^{\bullet} + e^- \rightarrow HO^-_{2(aq)} \quad [16]$$

They concluded that adsorption is critical to increasing the reduction rate by accelerating protonation of $O_2^{\bullet -}$ (Eq. 14). If $O_2^{\bullet -}$ becomes more basic upon adsorption, protonation and subsequent disproportionation or reduction of $HO_2^{\bullet}$ are accelerated.

Besides the controversy in the rate-determining step, the role of surface oxides is also poorly understood. Fagan *et al.*[27] and Zhang *et al.*[17] concluded that *o*-quinone-like structures are possible candidates to catalyze the reduction of oxygen. Evans and Kuwana suggested that the oxygen-containing groups may serve as mediators

* Electrochemical Society Active Member.
z E-mail: mccreery.2@osu.edu

S0013-4651(99)12-021-4 CCC: $7.00

between the electrode and the electroactive species.[28] Hossain *et al.* have observed oxygen reduction catalysis by adsorbed phenanthrenequinone in base, under conditions where the semiquinone anion (PQ^-) is formed.[9] They proposed that adsorbed PQ^- catalyzes oxygen reduction on a highly ordered pyrolytic graphite (HOPG) basal plane

$$PQ_{(ads)} + e^- \rightleftarrows PQ^-_{(ads)} \quad [17]$$

$$PQ^-_{(ads)} + O_2 \rightleftarrows PQ_{(ads)}\cdots\cdots O_2^- \quad [18]$$

$$PQ_{(ads)}\cdots\cdots O_2^- + H_2O + e^- \rightleftarrows PQ_{(ads)} + HO_2^- + OH^- \quad [19]$$

Nagaoka *et al.*[18] studied oxygen reduction at anodized GC electrodes and GC surfaces with adsorbed quinones. They observed that potentials of the O_2 reduction on anodized GC were pH independent, whereas those for quinone adsorbed on GC shifted negative at a rate of −60 mV per pH, characteristic of a quinone/hydroquinone reaction. If the quinone mediates the O_2 reduction, then the O_2 wave should also be pH dependent on anodized GC. Thus, they argued that quinone catalysis is possible, but unlikely for oxidized carbon surfaces unmodified by quinone adsorption.

Although there is general agreement that superoxide is an intermediate in the ORR on carbon, its adsorption and eventual fate are not clear. The $O_2/O_2^{\bullet -}$ couple is chemically reversible on carbon in nonaqueous solvents, but superoxide rapidly decays in water, and a peak for electrogenerated $O_2^{\bullet -}$ is rarely observed. Xu, *et al.* observed a small anodic peak corresponding to $O_2^{\bullet -}$ oxidation in 1 M tetraethylammonium hydroxide,[12] and Choi *et al.* observed a chemically reversible voltammogram for O_2 reduction in 1 M KOH on GC modified with a cobalt "disalophen" complex.[24] They attributed the observed $1e^-$ reduction to the $O_2/O_2^{\bullet -}$ couple, with $O_2^{\bullet -}$ stabilized by interaction with the cobalt complex.

The current work is directed at establishing the nature of the interaction between carbon surfaces and oxygen which leads to electrocatalytic formation of HO_2^- in the absence of transition metals. The approach exploits chemical modifications of the carbon surface which have been shown to suppress adsorption of simpler redox systems such as methylene blue and chlorpromazine.[29] In addition, a recently developed pretreatment of GC surfaces[30] was used to make GC electrodes which are unusually reactive toward peroxide formation from oxygen. By examining the opposing extremes of a highly surface-active GC surface and one for which adsorption is suppressed, interactions between the carbon surface and oxygen reduction intermediates were revealed, thus providing new insights into the ORR mechanism.

Experimental

Reagents.—Tetrabutylammonium tetrafluoroborate (NBu_4BF_4), 50% fluoboric acid, and *p*-toluidine were purchased from Aldrich Chemical Company and were used as received. Sodium nitrite was purchased from Sigma Chemical Company and used as received. 1 M KOH was made using preboiled Nanopure water and low carbonate KOH pellets. H_2O_2 solution was made from a 30% H_2O_2 stock (Fisher Scientific). Phosphate-buffered saline solution (0.9 M KCl, 0.1 M total phosphate, pH 7) was prepared from $K_2HPO_4{\cdot}3H_2O$ (reagent grade, J. T. Baker), KH_2PO_4 (reagent grade, J. T. Baker), KCl (reagent grade, J. T. Baker), and by adding KOH (Mallinckrodt) to the desired pH. Borate buffer (0.9 M KCl, 0.1 M total borate, $8 < pH < 12$) solution was prepared from H_3BO_3 (reagent grade, J. T. Baker), KCl, and by adding KOH to the desired pH. Acetate buffer solution (0.9 M KCl, 0.1 M total acetate, pH 4) was prepared from CH_3COOH (reagent grade, J. T. Baker), KCl, and by adding KOH to the desired pH. All electrolytes were made fresh before use. The tetrafluoroborate salt of 4-methylphenyl diazonium ion was synthesized according to the procedure described by Starkey *et al.*[31] with minor modifications[29] 0.1 mol of the *p*-toluidine was dissolved in 44 mL of 50% fluoboric acid. The solution was placed in an ice bath and stirred with an efficient stirrer, then a cold solution of 0.1 mol of sodium nitrite in 14 mL of water was added dropwise. When the addition was complete, the mixture was stirred for several more minutes and then suction filtered on a sintered glass filter. The solid diazonium tetrafluoroborate was washed with cold fluoboric acid, ethanol, and ether. The product, its NMR, and mass spectroscopy data are given as follows:
4-methylbenzenediazonium fluoborate, NMR (d_6-DMSO, 250 MHz): $\delta = 2.59$ (s, 3H), 7.81, 8.56 (d, 4H, $J = 8.45$ Hz), MS (FAB) calcd for $C_7H_7N_2$ *m/z* 119.15, found *m/z* 119.07 $(M\text{-}BF4)^+$.

Electrode materials and preparation.—Commercial GC 20 electrodes from Bioanalytical Systems Inc. (MF2070) of 0.071 cm^2 area were used in this work. Before any modification procedures, the electrodes were polished successively in 1, 0.3, and 0.05 μm alumina power (Buehler) slurries with Nanopure water (Barnstead) on microcloth polishing cloth (Buehler) and subsequently washed and sonicated in Nanopure water for 10 min. Activated electrodes were prepared by sonication in a suspension of activated carbon (AC) in isopropyl alcohol; these are referred to as IPA/AC electrodes.[30] Electrodes were polished conventionally and then were sonicated for 10 min in a 1/3 (v/v) mixture of Norit AC and reagent grade isopropanol (Mallinckrodt). The IPA/AC mixture was covered and allowed to stand for 30 min before use. After sonication in IPA/AC, the electrode was sonicated for an additional 10 min in Nanopure water. Chemisorption of methylphenyl radicals on GC surfaces was accomplished by the reduction of the diazonium salt in acetonitrile containing 0.1 M NBu_4BF_4 for 10 min at −0.57 V *vs.* Ag/Ag^+. Due to the robust C-C bond formed during diazonium modification, the modified GC electrodes are stable for at least several days. However, electrodes were used for ORR studies within a few hours of preparation.

Electrochemical measurements.—Cyclic voltammetry was performed in a conventional three-electrode cell with an Ag/AgCl/3 M KCl reference electrode and Pt auxiliary electrode, using a Bioanalytical Systems BAS 100 potentiostat. The electrolyte was saturated with argon (Linde Gas, prepurified) or oxygen (Linde Gas, ultrahigh purity) for 20 min prior to voltammetry. During data acquisition, the purging gas was passed above the solution without disturbing it. The saturated concentration and the diffusion coefficient of the oxygen were assumed to equal the established values of 1.0 mM[1] and 1.65×10^{-5} cm^2/s,[32] respectively.

Results and Discussion

The effect of methylphenyl modification of GC on the voltammetry of dissolved O_2 is shown in Fig. 1 and 2. The most surprising result occurs at pH 14, where the modified surface exhibits a chemically reversible redox couple, which becomes less reversible as the pH is decreased. In addition, the IPA/AC pretreatment yields a larg-

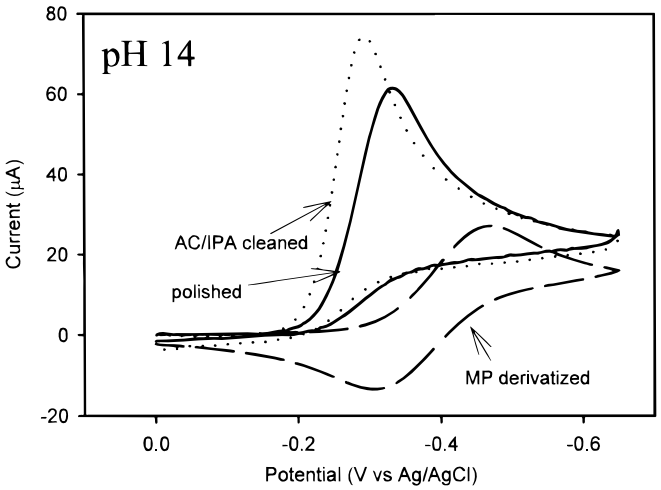

Figure 1. Voltammograms of O_2-saturated 1M KOH on GC electrodes, 200 mV/s. MP refers to a GC surface with a covalently bonded monolayer of methylphenyl groups. Background current was subtracted.

S0013-4651(99)12-021-4 CCC: $7.00

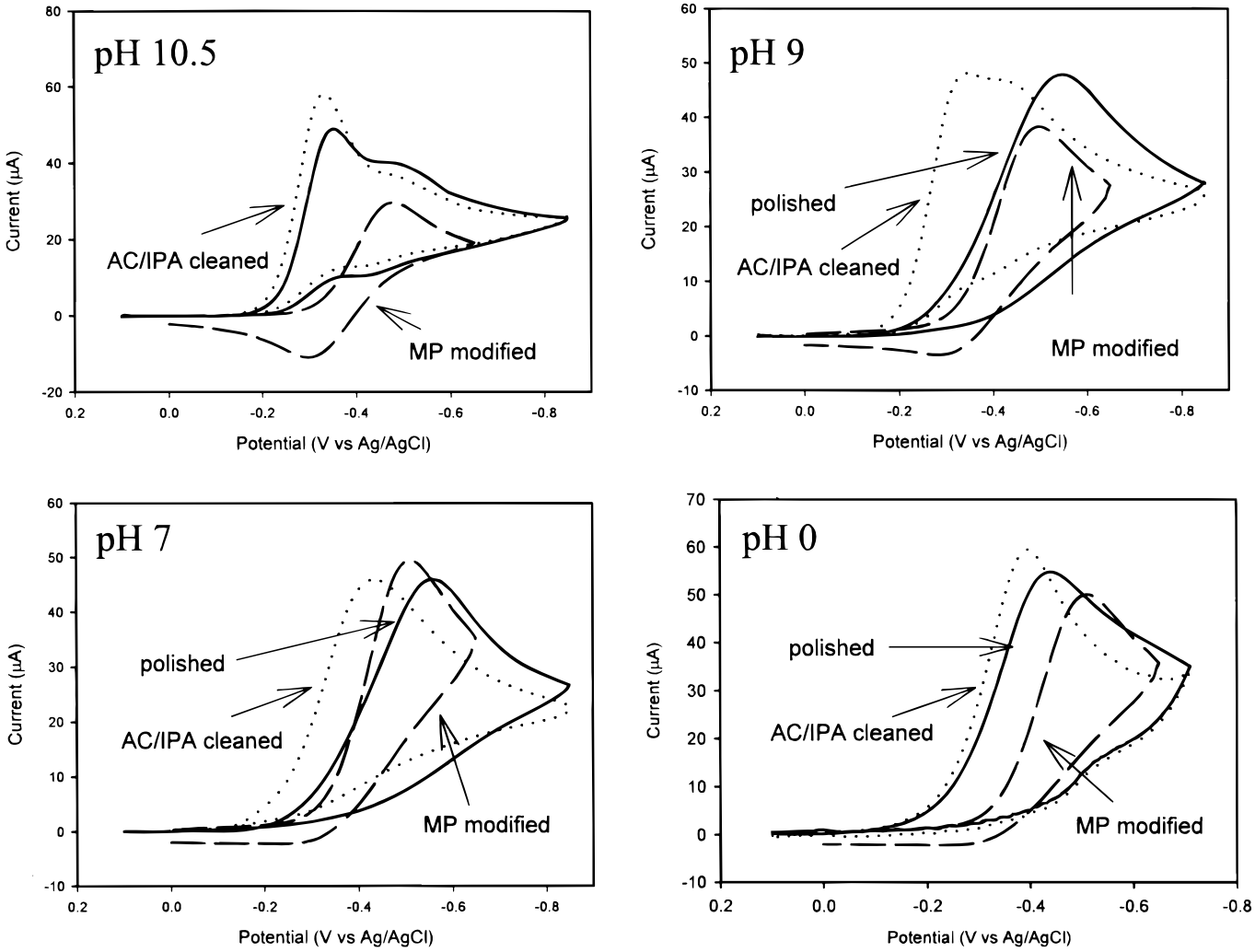

Figure 2. Voltammograms of O_2 reduction at four pH values. Same conditions as Fig. 1, but pH 9 and 10.5 were in borate buffer, pH 7 in phosphate, and pH 0 in 1 M H_2SO_4. Background current was subtracted.

er, more positive reduction wave compared to the polished surface. Figure 3 shows the voltammetry of 3 mM H_2O_2 at pH 14 on polished and modified GC. Neither surface reduces HO_2^- in the potential range shown, and both exhibit comparable HO_2^- oxidation waves. For the modified surface, the O_2 generated by HO_2^- oxidation is reduced on the subsequent scan, again exhibiting chemical reversibility. On polished GC, the reduction of electrogenerated O_2 is similar to that observed for an O_2 solution at the same pH.

Figures 1 through 3 demonstrate a profound change in O_2 reduction chemistry on the methylphenyl (MP)-modified surface compared to either the polished or IPA/AC-treated surface. Although unexpected, the reverse wave on the modified surface implies formation of superoxide ion, which is stable at pH 14 on the voltammetric time scale. As noted earlier, the MP modification should prevent adsorption of O_2 or its reduction products on the carbon surface, causing a dramatic effect on O_2 voltammetry. To understand the more complex voltammetry on the unmodified GC surface, MP-modified GC was studied in some detail. After describing the results and conclusions for the modified surface, the unmodified GC is revisited in greater detail.

MP-modified GC.—Figure 4 shows the scan rate dependence of the O_2 reduction wave on modified GC at pH 14. Both the reduction and oxidation peak heights show a linear dependence on $\nu^{1/2}$, and ΔE_p increases with the scan rate. The slope of i_p *vs.* $\nu^{1/2}$ for the reduction peak on the MP-modified GC is about half that of the polished surface, and corresponds to that expected for a one-electron reduction. Both i_p^c and i_p^a track $\nu^{1/2}$, implying chemical reversibility over the time scale of 0.5 to 10 s. These observations are consistent with a $1e^-$ reduction of O_2 to $O_2^{\bullet -}$, without adsorption and with a k^o of approximately 0.003 cm/s. Table I shows voltammetric results for

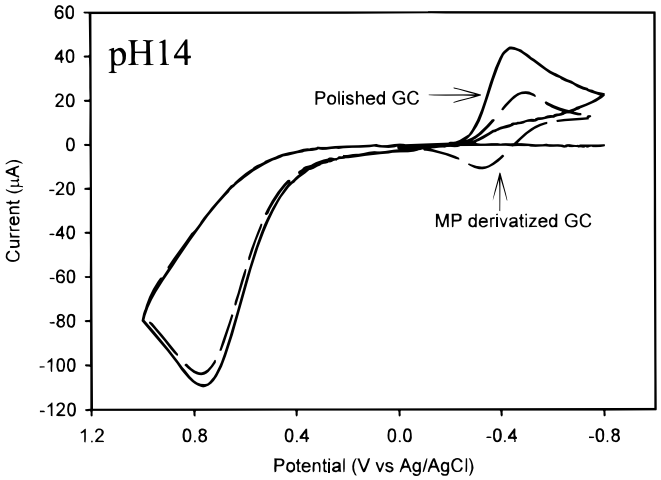

Figure 3. Voltammetry of 3 mM H_2O_2 in 1 M KOH on polished and MP-modified GC. Scans were initiated at −0.8 V, and were stopped at 0 V after about 1.3 cycles. Background current was subtracted.

S0013-4651(99)12-021-4 CCC: $7.00

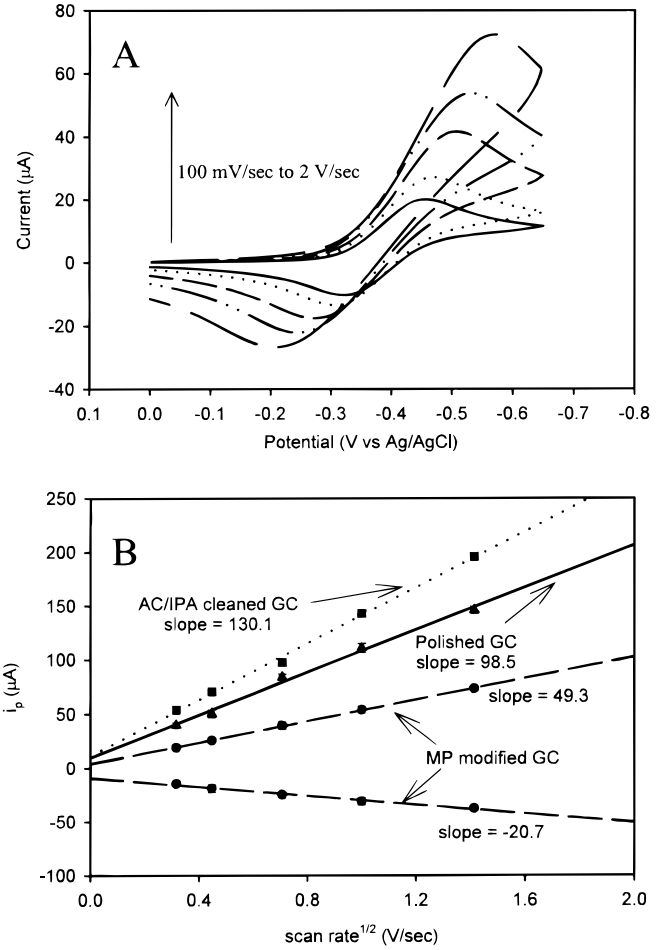

Figure 4. Scan rate dependence of voltammetry on MP-modified GC for the range of 0.10 to 2.0 V/s. (B) Plots of i_p *vs.* $\nu^{1/2}$ for the reduction and oxidation waves, compared to polished and IPA/AC-treated electrodes. The lower line is the anodic peak current; the remaining three are the cathodic peak current.

0.1 to 2.0 V/s and three pH values, along with k^o values determined from ΔE_p. Reverse voltammetric peaks were observed at pH 12-14, and results for three pH values are shown. Both $E^{1/2}$ (determined from the average of E_p^a and E_p^c) and k^o (determined from ΔE_p) show minor changes with pH and scan rate. The means and standard deviations of 45 determinations for five scan rates and three pH values are $E_{1/2} = -0.381 \pm 0.004$ V *vs.* Ag/AgCl and $k^0 = 0.0031 \pm 0.005$ cm/s. Since reversible voltammograms for O_2 reduction to $O_2^{\bullet-}$ are rarely observed, there are few values in the literature for $E_{1/2}$ and k^o. From thermodynamic data, the E^o for $O_2/O_2^{\bullet-}$ is -0.33 V *vs.* normal hydrogen electrode (NHE), for unit activity of $O_2^{\bullet-}$ and 1 atm of O_2. [1] The electrochemical $E_{1/2}$ occurs when $[O_2] = [O_2^{\bullet-}]$, assuming equal diffusion coefficients. Since $[O_2]$ is initially 1 mM for 1 atm O_2, rather than unit activity, $E_{1/2}$ is predicted to be positive of E^o by 0.0591 log 10^3, *i.e.*, $E_{1/2} = -0.153$ V *vs.* NHE or -0.358 V *vs.* Ag/AgCl.[33] Choi, *et al.*[24] observed $E_{1/2} = -0.21$ V *vs.* Ag/AgCl on modified GC, and Xu, *et al.* observed -0.325 V in 1 M tetraethylammonium hydroxide. Chevalet *et al.*[33] report -0.316 V *vs.* Ag/AgCl for a quinoline-modified mercury electrode. Some of this variation is due to the strong dependence of the $O_2/O_2^{\bullet-}$ potential on the medium.[1] Nevertheless, the $E_{1/2}$ value on MP modified is within 30 mV of that expected from thermodynamic data.

As observed for several outer-sphere redox systems such as $Ru(NH_3)_6^{+3/+2}$ [34] and methyl viologen$^{+2/+1}$,[29] a thin monolayer on GC has a minor effect on the observed electron-transfer rate constant for O_2 reduction to superoxide. For a nitrophenyl monolayer, a decrease in k^o of a factor of 2 was observed for chlorpromazine, methyl viologen, and $Ru(NH_3)_6^{+3/+2}$, consistent with electron tunneling through the monolayer.[29] The k^o of $O_2/O_2^{\bullet-}$ on bare GC was estimated as 0.005 cm/s in a previous report, based on a small reverse wave observed in tetraethylammonium hydroxide electrolyte.[12] The methylphenyl modification used in the current work exhibits a k^o of 0.003 cm/s, consistent with outer-sphere electron transfer to the $O_2/O_2^{\bullet-}$ couple through a methylphenyl monolayer.

Table I. $E_{1/2}$, ΔE_p, and k^0 for dioxygen reduction on methylphenyl derivatized GC.

	Scan rate (V/s)	$E_{1/2}$ (mV)	ΔE_p (mV)	[a]k^0 (cm/s)
	0.1	−382 ± 3	145 ± 5	0.0035 ± 0.0003
	0.2	−381 ± 2	172 ± 3	0.0035 ± 0.0002
pH 14	0.5	−383 ± 2	230 ± 3	0.0032 ± 0.0003
	1	−380 ± 4	264 ± 6	0.0032 ± 0.0005
	2	−379 ± 5	314 ± 8	0.0028 ± 0.0008
	0.1	−381 ± 4	147 ± 6	0.0033 ± 0.0004
	0.2	−382 ± 2	171 ± 3	0.0035 ± 0.0002
pH 13	0.5	−378 ± 3	235 ± 5	0.0030 ± 0.0005
	1	−382 ± 5	270 ± 8	0.0028 ± 0.0007
	2	−383 ± 7	318 ± 9	0.0029 ± 0.0010
	0.1	−382 ± 4	146 ± 7	0.0032 ± 0.0005
	0.2	−379 ± 5	172 ± 5	0.0035 ± 0.0004
pH 12	0.5	−381 ± 2	237 ± 3	0.0029 ± 0.0003
	1	−380 ± 5	271 ± 9	0.0028 ± 0.0008
	2	−378 ± 6	320 ± 8	0.0029 ± 0.0008

[a] Mean ± standard deviation for three determinations.

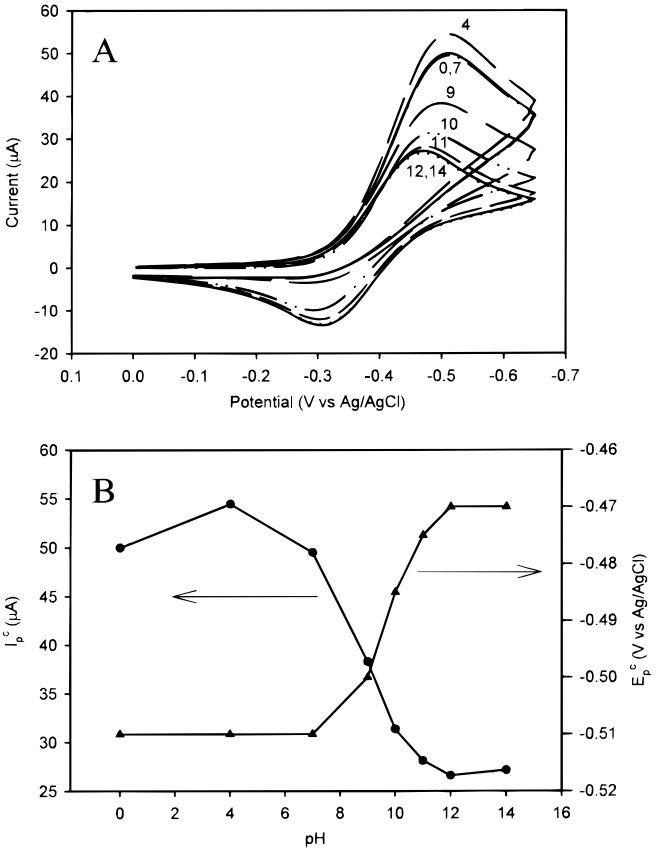

Figure 5. (A) Dependence of O_2 voltammetry on MP-modified GC as a function of pH, all at 200 mV/s in O_2-saturated solutions. (B) Changes in cathodic peak current and potential with pH.

S0013-4651(99)12-021-4 CCC: $7.00

The pH dependence of O_2 voltammetry on MP-modified GC is shown in Fig. 5a, and the trends of E_p and i_p are shown in Fig. 5b. As the pH is decreased, i_p increases by approximately a factor of 2 while E_p shows minor variations (~40 mV). The lack of a pH dependence of E_p indicates no proton transfers are involved in the initial reduction reaction, consistent with electrogeneration of $O_2^{\bullet -}$ at ~ −0.5 V *vs.* Ag/AgCl.

The decrease in the reverse wave in Fig. 5 as the pH is lowered is likely caused by the instability of superoxide ion in acidic or neutral solution. Superoxide reactions have been studied in detail with pulse radiolysis. Bielski and Allen,[35] concluded a two-step mechanism

$$O_2^{\bullet -} + H_2O \leftrightarrows HO_2^{\bullet} + OH^- \quad [20]$$

$$HO_2^{\bullet} + O_2^{\bullet -} \leftrightarrows HO_2^- + O_2 \quad [21]$$

They combined Reactions 20 and 21 into a disproportionation

$$2\ O_2^{\bullet -} + H_2O \leftrightarrows O_2 + HO_2^- + OH^- \quad [22]$$

with an equilibrium constant K_{22} of 1008 and an observed rate constant of $5 \times 10^{(12\text{-pH})}$ above pH 6. If one assumes that the modified electrode serves only to generate $O_2^{\bullet -}$ from O_2 and does not adsorb or react with O_2 reduction products, the disproportionation of $O_2^{\bullet -}$ depicted in Reaction 22 should occur in homogeneous solution.

Commercial stimulation software[36] was used to calculate voltammograms for O_2 reduction on MP-modified GC, according to Reactions 22 and 23

$$O_2 + e^- \leftrightarrows O_2^{\bullet -} \quad E^o = -0.38\text{V},\ k^o = 0.003\ \text{cm/s} \quad [23]$$

The observed rate for Reaction 22 is pH dependent,[35] according to Eq. 24

$$k_{obsd} = \frac{(7.6 \times 10^5) + (1.58 \times 10^{pH+3})}{(1 + 1.78 \times 10^{pH-5})^2} \quad [24]$$

For pH > 6, the initial terms in the numerator and denominator of Eq. 24 become negligible, and $k_{obsd} = 5 \times 10^{12\text{-pH}}$. The homogeneous decay of $O_2^{\bullet -}$. in water is controlled by the reaction of $HO_2^{\bullet}$ with $O_2^{\bullet -}$, and the pH dependence arises from the $HO_2^{\bullet}/O_2^{\bullet -}$ equilibrium. Comparison of simulated voltammograms based on Reactions 22 and 23 and Eq. 24 are shown in Fig. 6. The good agreement between theory and experiment support the mechanism of Reactions 22 and 23, with the decay of O_2^- occurring totally in homogeneous solution. Furthermore, the slope of the plot of i_p *vs.* $\nu^{1/2}$ for the simulated curves (54.9 μA $s^{1/2}$ $V^{-1/2}$) is close to the observed value for the MP-modified surface at pH 14 (49.3 μA $s^{1/2}$ $V^{-1/2}$). Note that literature values were used for the diffusion coefficient of oxygen and the rate of Reaction 22, and the only adjustable parameters in the simulation

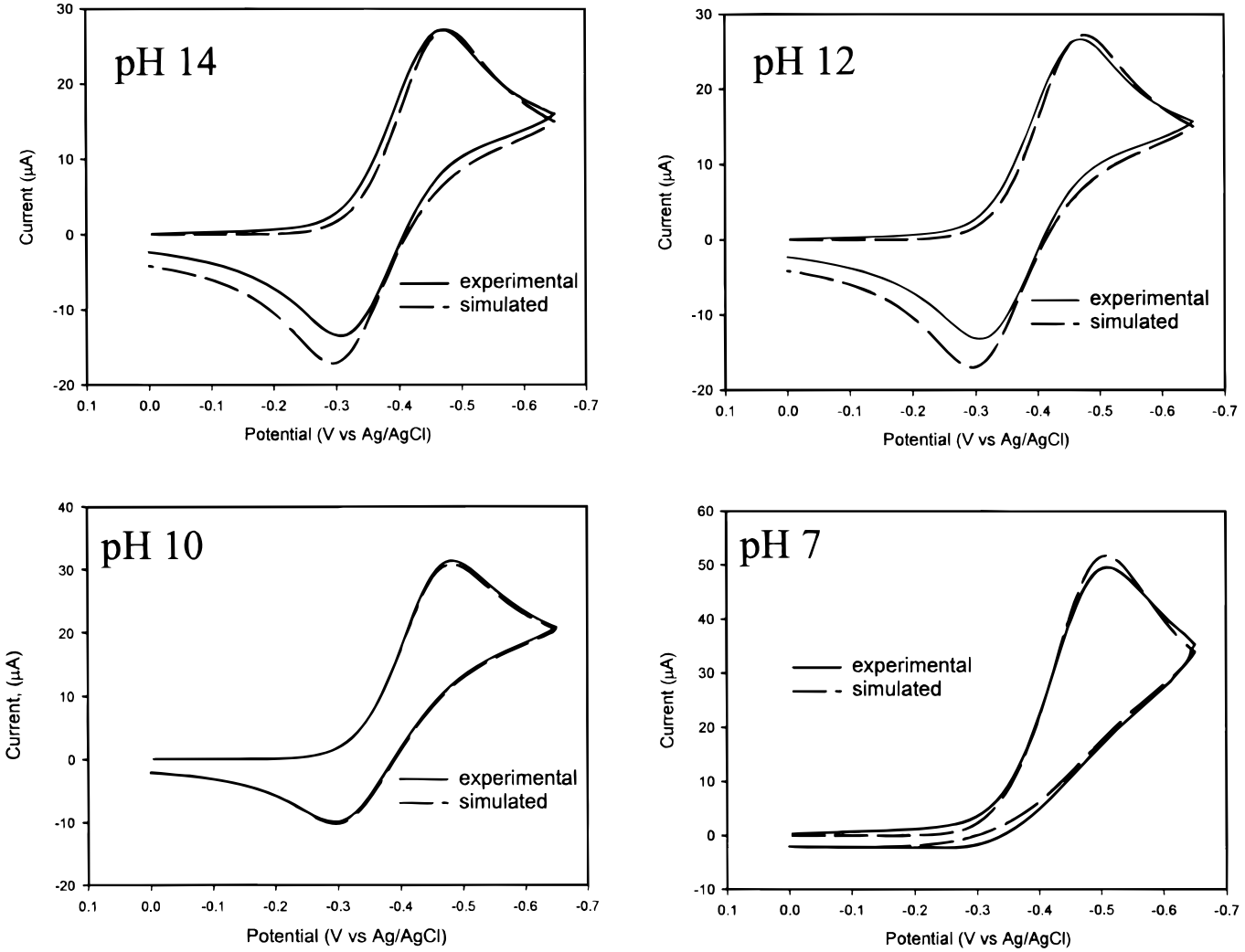

Figure 6. Comparison of observed (solid) and simulated (dashed) voltammograms for the mechanism of Reactions 22 and 23, after subtraction of background from experimental voltammograms. Simulations used $E_{1/2} = -0.381$ V, $k^o = 0.003$ cm/s, $= 0.5$, $A = 0.07$ cm^2, $C^b = 1$ mM, $D = 1.6 \times 10^{-5}$ cm^2/s, and $\nu =$ 0.20 V/s. The rate of Reaction 22 varied with pH, according to Eq. 24.

S0013-4651(99)12-021-4 CCC: $7.00

were k^o and α. Although chemical reversibility for the $O_2/O_2^{\bullet-}$ redox system at pH > 10 is very unusual, it is not surprising once the consequences of the pulse radiolysis results are appreciated. At pH 14, k_{obsd} is predicted by Eq. 24 to be 0.05 M^{-1} s^{-1}. The initial decay rate of $O_2^{\bullet-}$ is predicted to be 5×10^{-8} M s^{-1} for 1 mM $O_2^{\bullet-}$ and it would require about 30 min for 10% of the $O_2^{\bullet-}$ to decay via Reaction 22. At pH 10, 10% of the $O_2^{\bullet-}$ reacts in about 200 ms, but that is still slow enough to observe an anodic peak for $O_2^{\bullet-}$ oxidation (Fig. 6). The discrepancy between simulation and experiment for the anodic peaks in Fig. 6 for pH 12 and 14 appears to be pH independent and may be due to disproportionation of unprotonated $O_2^{\bullet-}$ or to reactions of $O_2^{\bullet-}$ with residual solvent impurities. The rate constant for disproportionation of unprotonated $O_2^{\bullet-}$ has been reported as <0.3 M^{-1} s^{-1}. [35] A critical conclusion from the MP-modified electrode is that the irreversibility of O_2 depends directly on the presence of adsorption sites on the GC surface. If the interaction between $O_2^{\bullet-}$ and the electrode is blocked by MP groups, the $O_2^{\bullet-}$ is relatively stable. In the absence of surface interactions, the electrogenerated superoxide decays by established routes in homogeneous solution. Chemical reversibility of the $O_2/O_2^{\bullet-}$ redox couple in aqueous base has been reported previously on mercury electrodes modified with a thin film of a quinoline derivative,[33,37] but the effect was attributed to formation of a nonaqueous phase on the electrode surface which stabilized $O_2^{\bullet-}$. Since the MP layer is only about 5 Å thick, a phase separation model is difficult to envision for MP-modified GC electrodes.

Unmodified GC.—When the MP monolayer is not present, O_2 or superoxide adsorption sites depend strongly on surface pretreatment, leading to potential variability in voltammetric observations. Figure 1 demonstrated that solvent cleaning with isopropanol and AC alters O_2 voltammetry significantly, presumably by removing impurities and increasing the number of adsorption sites. In separate reports, we showed that the IPA/AC solvent treatment yielded unusually clean and reactive GC surfaces, and high physisorption of catechols and methylene blue.[30,38] The polished and IPA/AC-treated surfaces are compared here because they provide insight into the role of adsorption in O_2 reduction.

Figure 7 shows an overlay of voltammograms for O_2 reduction on polished GC at several pH values. As reported by Taylor and Humffray,[16] the voltammograms exhibit a very unusual pH dependence, with the more positive reduction peak decreasing in height with decreasing pH, and a peak developing at *ca.* −0.55 V which shifts very slightly with pH. On the IPA/AC-pretreated GC surface, the relative size of the more positive reduction peak increases, as shown in Fig. 2. Figure 8 shows that the relative magnitudes of the two reduction peaks observed at pH 10.5 depend on the scan rate, with the more positive peak decreasing in relative size as the scan rate is increased.

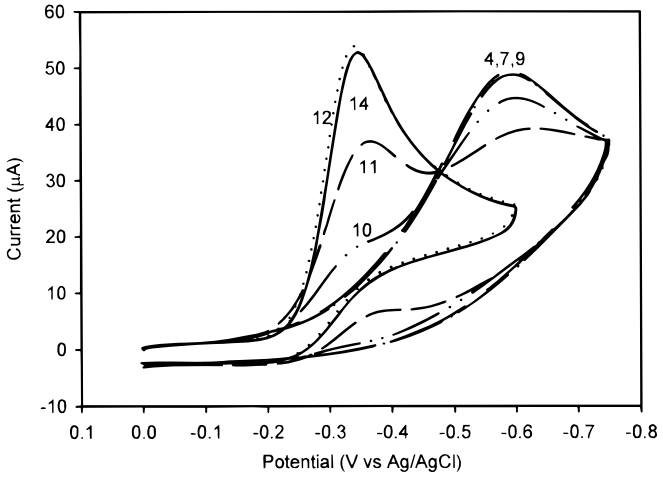

Figure 7. Voltammetry of O_2 reduction on polished GC as a function of pH, same conditions as Fig. 1. Electrode was repolished before each run.

Several conclusions are possible from the results which lead to a plausible O_2 reduction mechanism on unmodified GC. First, the voltammetric peak currents imply an overall $2e^-$ reduction as expected from many reports that H_2O_2 or HO_2^- is the reduction product. Even when two reduction peaks are apparent (as at pH 9 or 10.5), their heights imply two electrons, rather than one or four. The slope of the i_p *vs.* $v^{1/2}$ for pH 14 on IPA/AC-treated electrodes is 130 μA $s^{1/2}$ $V^{-1/2}$, close to the value of 122 calculated for irreversible electron transfer with $n = 2$ and $\alpha n = 0.5$. Second, both reduction potentials are nearly pH independent, although their relative magnitudes change markedly between pH 12 and 7. Third, the more positive peak potential for the initial O_2 reduction on unmodified GC is consistent with our previous conclusion attributing it to Reaction 23.[12] Adsorption of $O_2^{\bullet-}$ is more pronounced on IPA/AC-treated GC (hence the more positive E_p), and is prevented altogether on MP-modified GC. Fourth, the more negative of the two reduction peaks observed near pH 10 exhibits a reverse wave at ~ −0.43 V *vs.* Ag/AgCl. Consider the mechanism of the earlier Reactions 13, 14, and 16. We proposed previously that adsorption of $O_2^{\bullet-}$ increases its pK_a from 4 to perhaps 9, making Reaction 14 more favorable.[12] It is possible that $HO_{2ads}^{\bullet}$ could react with $HO_2^{\bullet}$ or $O_2^{\bullet-}$, possibly themselves adsorbed, to yield H_2O_2 and O_2. However, an important alternative arises when we consider the nature of $HO_{2ads}^{\bullet}$. If $HO_{2ads}^{\bullet}$ binds to a surface radical site, the product is electronically identical to an aryl hydroperoxide of the general formula R-O-O-H. Each oxygen has an octet of electrons, and the *t*-butyl analog is stable in water. According to Das *et al.*, the pK_a of hydroperoxides ranges from 8.9 to 12.8, and is 8.9 for C_6H_5OOH.[39] If C_6H_5OOH is a reasonable analog of $HO_{2ads}^{\bullet}$, then the increase in the pK_a of the $O_{2ads}^{\bullet-}/HO_{2ads}^{\bullet}$ acid base pair explains the increased rate of Reaction 14 for $O_{2ads}^{\bullet-}$ compared to $O_2^{\bullet-}$(aq). Note that Reaction 14 is the same as that concluded by Allen and Bielski for $O_{2(aq)}^{\bullet-}$, except that it applies to adsorbed $O_2^{\bullet-}$. Application of the steady-state approximation to Reactions 13, 14, and 16 leads to Eq. 25 as the rate law for generation of $HO_{2(aq)}^-$

$$\frac{d[HO_2^-]}{dt} = \frac{k_{13}k_{14}k_{16}[O_2]}{k_{14}k_{16} + k_{-13}k_{16} + k_{-13}k_{-14}[OH^-]} \qquad [25]$$

Note that k_{13}, k_{-13}, and k_{16} are potential dependent, and Reaction 16 is assumed to be irreversible. Definition of k_{obsd} as the collection of rate constants in Eq. 25, and rearrangement yields

$$\frac{1}{k_{obsd}} = \frac{1}{k_{13}} + \frac{1}{K_{13}k_{14}} + \frac{[OH^-]}{K_{13}K_{14}k_{16}} \qquad [26]$$

If the first term on the right side of Eq. 26 is much larger than the other two, Reaction 13 is the rate-determining step (rds), and if the middle term on the right side of Eq. 26 is dominant, then Reaction 14 is the rds. The potential dependence of k_{obsd} may be predicted by substituting Butler-Volmer expressions for k_{13}, k_{-13}, and k_{16}, and considering the cases when Reactions 13, 14, or 16 are rate limiting. For example, if Reaction 13 is the rds, $k_{obsd} = k_{13}$, and

$$k(E) = k_{13}^0 \exp[-f\alpha_{13}(E - E_{13}^0) \qquad [27]$$

where $f = F/RT$, and k_{13}^0, α_{13}, and E_{13}^0 all refer to the reduction of O_2 to $O_{2ads}^{\bullet-}$. Table II lists the predicted rate expressions for the three extremes in which one reaction is rate limiting. Note that when reaction 14 is rate limiting, Reaction 13 acts as a pre-equilibrium which follows the Nernst equation. Also shown in Table II is the apparent transfer coefficient expected for the potential dependence of k_{obsd}.

A similar analysis was applied by Hu and Kuwana[40] and Deakin *et al.*[41] to the successive electron transfers accompanying ascorbic acid and catechol oxidation. Semi-integral analysis was used to determine a_{obsd} as a function of potential. Semi-integrals of the voltammograms of four different pH values are shown in Fig. 9a and plots of $\ln[i(t)/(I_l - I(t))]$ *vs.* E are shown in Fig. 9b. The slope of the lat-

S0013-4651(99)12-021-4 CCC: $7.00

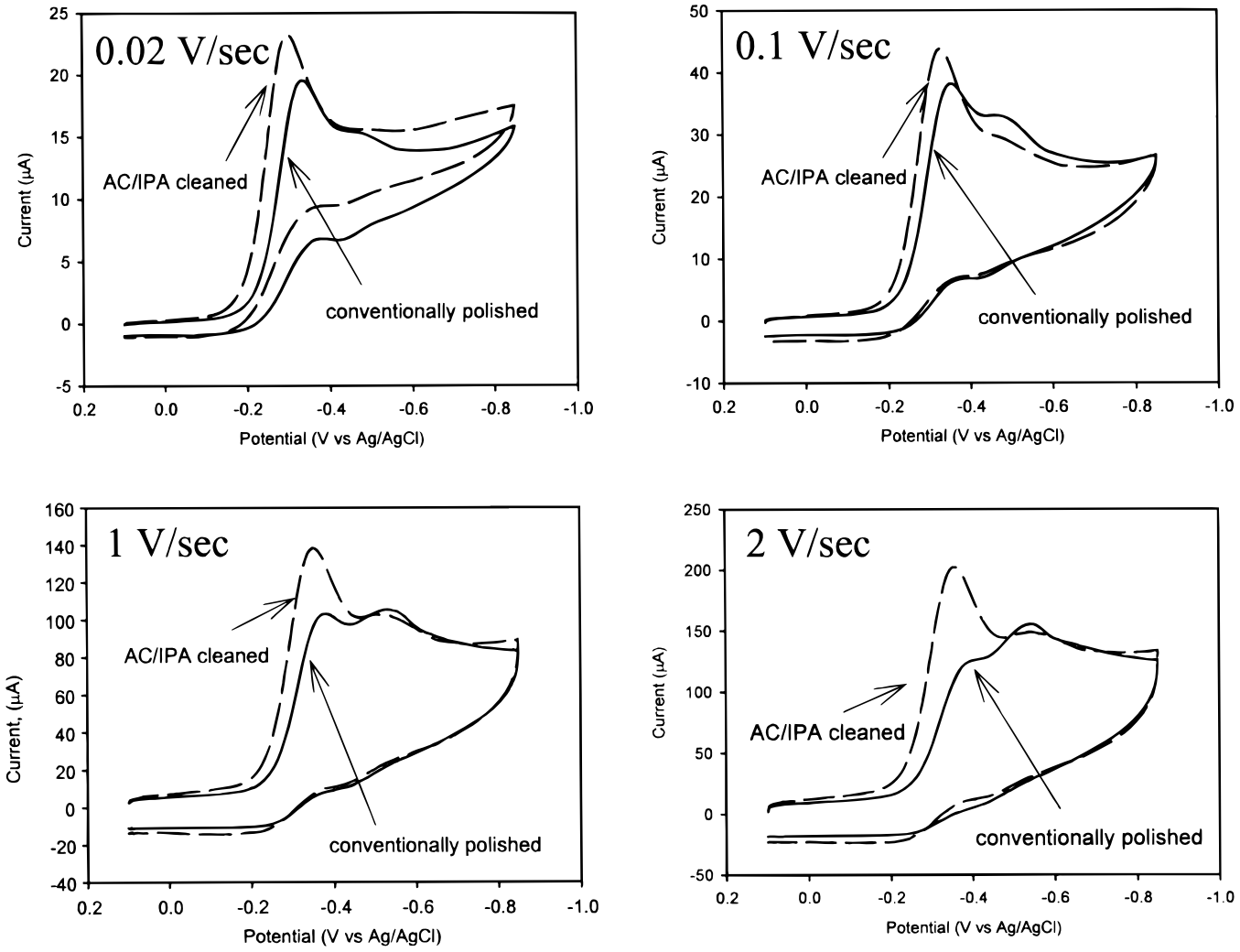

Figure 8. Scan rate dependence of O_2 reduction voltammetry on polished and IPA/AC-treated GC. pH was 10.5 with borate buffer (0.1 M) in 0.9 M KCl. Electrode was freshly prepared before each run.

ter plots equals an *F/RT*, [42] and permits evaluation of the transfer coefficient as a function of potential. Table III lists α_{obsd} for the four cases shown in Fig. 9. The semi-integrals for the MP-modified surface are consistent with slow electron transfer to form soluble $O_2^{\bullet -}$, which is stable above pH 12. At lower pH, α_{obsd} remains at 0.5, although the homogeneous reaction increases the total number of electrons from one to two. For the IPA/AC surface at pH 14, α_{obsd} approaches 1.0, implying that Reaction 14 is the rds. If $HO_{2ads}^{\bullet}$ behaves like R-O-O-H, its pK_a is 10^{-9} and K_{14} is 10^{-5}. The reduction potentials for $RO_2^{\bullet}/RO_2H$ and $RO_2^{\bullet}/RO_2^-$ are expected be positive (1.3 to 1.8 V *vs.* NHE for C_6H_5OOH),[39] so the electrode is negative of the potential required to reduce $HO_{2ads}^{\bullet}$. Thus Reaction 16 is overdriven and probably fast compared to Reactions 13 and 14. An α_{obsd} of +1.0 and an rds of Reaction 14 is reasonable for a clean GC surface at pH 14.

As the pH is lowered, Reaction 14 accelerates, and the α_{obsd} for pH 10.5 or 9 is ~0.5 for the early part of the wave on the IPA/AC surface. This behavior is consistent with Reaction 13 becoming the rds, as Reaction 14 accelerates. The linearity of i_p with $\nu^{1/2}$ on the IPA/AC surface is also consistent with an overall $2e^-$ reduction to HO_2^-(aq), with the first electron transfer being rate limiting. The shift in rds from Reaction 14 to Reaction 13 as the pH is lowered from 14 to 10 explains the qualitative appearance of the voltammograms on the IPA/AC surface with the exception of the small couple between −0.4 and −0.5 V. This couple is likely due to the reduction of O_2 to $O_2^{\bullet -}$ without adsorption (Reaction 23). At lower pH, the adsorption sites on the GC surface may become saturated with $HO_{2\ ads}^{\bullet}$, thus blocking $O_2^{\bullet -}$ adsorption in Reaction 13. For $O_2^{\bullet -}$ adsorption, the clean GC surface at pH < 9 behaves like MP-modified GC, with the $O_2/O_2^{\bullet -}$ electron transfer being outer sphere. The small reverse wave at −0.4 V on IPA/AC GC is similar to the reverse wave observed on MP modified GC, but with faster electron-transfer kinetics. As the scan rate increases, the mass transport of O_2 to the surface is faster, and adsorption sites are more easily saturated. The

Table II. Predicted ionetic parameters for mechanism of Reactions 13, 14, and 16.

Rate-limiting step	k_{obsd}	Potential dependence of k_{obsd}	Apparent α
13	k_{13}	$k_{13}^o \exp[-\alpha_{13} f(E - E_{13}^o)]$	α_{13}
14	$K_{13}k_{14}$	$k_{14}^o \exp[-f(E - E_{13}^o)]$	1
16	$K_{13}K_{14}k_{16}/[OH^-]$	$K_{13}k_{14} \exp(fE_{13}^o + \alpha_{16} fE_{16}^o)] \exp[-f(1 + \alpha_{16})E]$	$1 + \alpha_{16}$

S0013-4651(99)12-021-4 CCC: $7.00

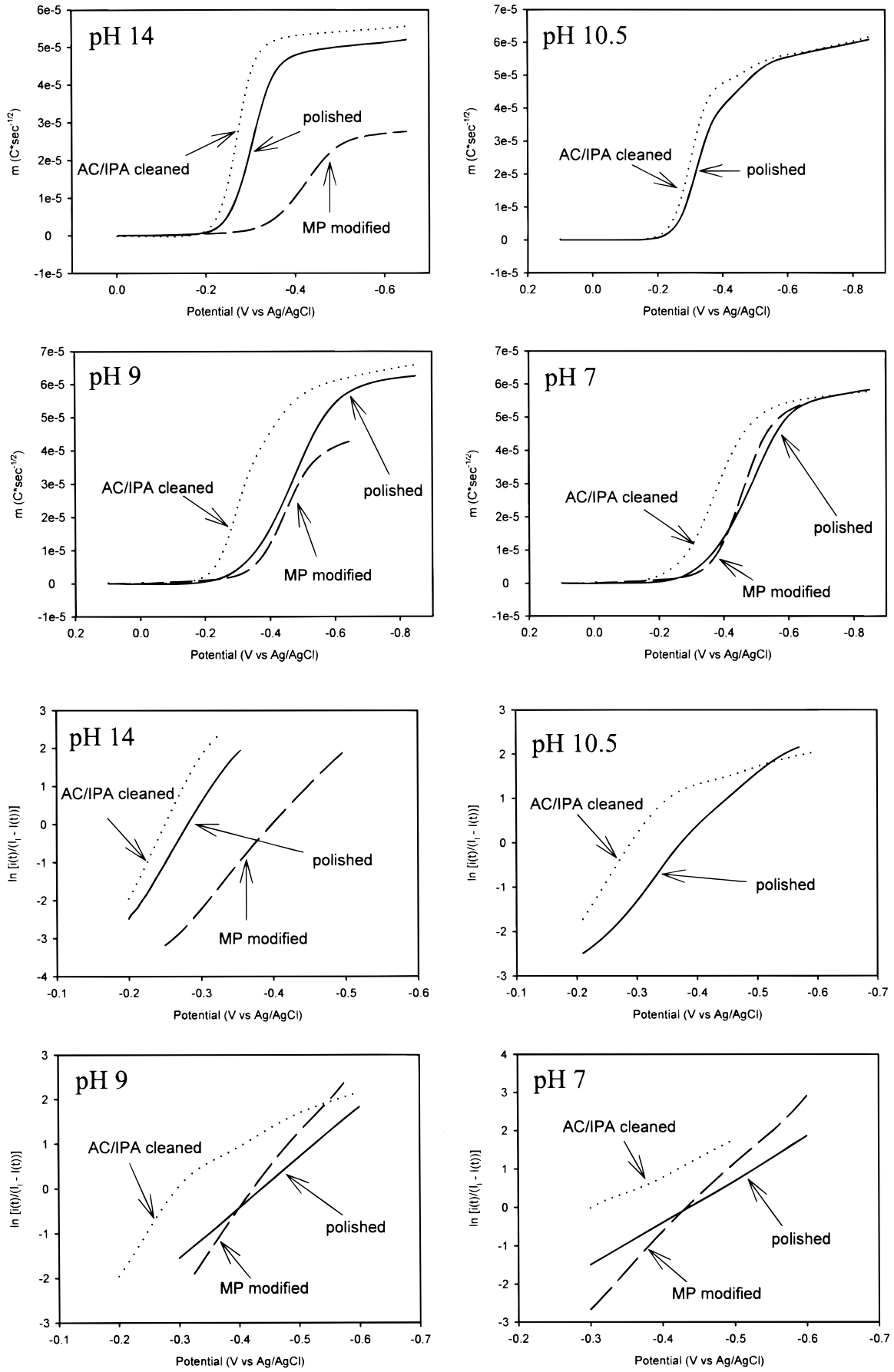

Figure 9. (A, top) Semi-integrals of background corrected reduction voltammograms for O_2 reduction at the electrodes and pH values indicated. (B, bottom) Plots of $\ln[i(t)/(I_1 - I(E))]$ *vs. E* from semi-integrals of (A).

S0013-4651(99)12-021-4 CCC: $7.00

Table III. Observed α for various conditions, from Fig. 9B.

pH	Polished	IPA/AC	MP
14	0.78	0.94	0.55
10.5	0.39[a] 0.29[b]	0.52[a] 0.11[b]	0.52
9	0.29	0.55[a] 0.18[b]	0.44
7	0.29	0.23	0.47

[a] Region between −0.2 and −0.3 V.
[b] Region between −0.4 and −0.5 V.

effect of scan rate is more pronounced on the polished surface, presumably because it has fewer adsorption sites to begin with. If the GC surface becomes saturated with HO_{2ads} below pH 9, the O_2 reduction mechanism on IPA/AC or polished GC is similar to that on the MP-modified surface, with $O_2^{\bullet-}$ degradation occurring primarily in homogeneous solution. At pH 7, 4, and 0, the differences in reduction peak potential appear to be due to differences in the electron-transfer rate for $O_2^{\bullet-}$ generation on the three surfaces. To further support this conclusion, simulations similar to those shown in Fig. 6 were repeated for Reactions 22 and 23 for a range of values of k^o for Reaction 23. At pH 7, with $k_{23} = 0.003$ cm/s, E_p^c is predicted to be −0.507 V *vs.* Ag/AgCl, consistent with the E_p^c observed on the MP modified surface. If k^o on the IPA/AC-treated surface increases to 0.01 cm/s, the simulated E_p^c shifts to −0.447 V, compared to an observed E_p^c on IPA-treated GC of −0.440 V. Therefore, in the absence of adsorption, the observations are consistent with the clean surface exhibiting a k^o which is about three times that of the MP surface, and saturation of adsorption sites on the IPA surface by adsorbed $\bullet O_2H$.

The nature of the adsorption site for $O_2^{\bullet-}$ is not obvious. The only certainty is the ability to block the site with an MP monolayer. Previous reports indicate that anodization of the surface increases the activity for O_2 reduction,[12] but it is not clear that surface oxides are involved, per se. O_2 reduction is indeed accelerated by surface oxidation or adsorbed quinones, but Reaction 14 appears to proceed on surfaces with low oxide coverage. For example, the IPA/AC-treatment decreases the O/C ratio of polished GC,[30] but accelerates O_2 reduction. A likely candidate for the adsorption site is a surface radical or "dangling bond." As noted earlier, adsorption of $O_2^{\bullet-}$ to a surface radical results in a relatively stable peroxide or hydroperoxide which is not a radical. The current results do not prove that a surface radical is the active site, but such a hypothesis is consistent with the observations.

Conclusions

The current results clarify the role of the carbon surface in the oxygen reduction mechanism. When the surface is blocked by an organic monolayer, the electrode serves only to reduce dioxygen to superoxide, with both remaining in aqueous solution. At a pH below about 10, the electrogenerated $O_2^{\bullet-}$ and $HO_2^{\bullet}$ disproportionate to O_2 and H_2O_2 by established homogeneous routes. The voltammograms on the MP-modified GC surface are quantitatively predictable from simulations based on Reactions 22 and 23, and Eq. 24. For this case, the MP monolayer prevents $O_2^{\bullet-}$ adsorption and leads to a relatively simple reduction mechanism.

When the GC surface is exposed by pretreatment with isopropanol and activated carbon, electrogenerated $O_2^{\bullet-}$ adsorbs to form a species which is electronically similar to a deprotonated hydroperoxide, ROO^-. This species is more basic than $O_2^{\bullet-}$(aq) and accepts a proton via Reaction 14. The critical consequence of $O_2^{\bullet-}$ adsorption is the increase in pK_a of $O_{2\,ads}^{\bullet-}$ compared to $O_2^{\bullet-}$(aq). The result is a change in rds from $O_2^{\bullet-}$ protonation (Reaction 14) for pH > 12 to O_2 reduction (Reaction 13) for pH < 10. As the pH is decreased to about 9, the adsorbed $O_2^{\bullet-}$ protonates to form a relatively stable hydroperoxide analog of ROOH. This species appears to occupy adsorption sites, thus preventing further $O_2^{\bullet-}$ adsorption. As a result, the O_2 reduction reverts to its outer sphere route without further adsorption. Although the surface is initially very active toward adsorption, an intermediate in the O_2 reduction process ($HO_{2ads}^{\bullet}$) rapidly blocks adsorption sites for a pH below 9. Except for somewhat faster electron transfer, the clean surface behaves like the MP-modified GC surface toward O_2 reduction below pH 9.

Acknowledgment

This work was supported by the Analytical and Surface Chemistry Division of the National Science Foundation.

Ohio State University assisted in meeting the publication costs of this article.

References

1. D. T. Sawyer, *Oxygen Chemistry*, Oxford University Press, London (1991).
2. R. Adzic, in *Electrocatalysis*, J. Lipkowski, and P. N. Ross, Editors, Chap. 5, Wiley-VCH, New York, (1998).
3. E. Yeager, *J. Mol. Catal.*, **38,** 5 (1986).
4. *Oxygen Electrochemistry*, J. Zagel, M. J. Aguirre, L. Busez, J. Pavez, F. C. Anson, and K. Kinoshita, Editors, PV 95-26, The Electrochemical Society Proceedings Series, Pennington, NJ (1996).
5. A. J. Appleby and J. Marie, *Electrochim. Acta.*, **24,** 1243 (1978).
6. J. Wang, N. Naser, L. Angnes, H. Wu, and L. Chen, *Anal. Chem.*, **64,** 1285 (1992).
7. P. A. Forshey and T. Kuwana, *Inorg. Chem.*, **22,** 699 (1983).
8. Y. O. Su, T. Kuwana, and S. M. Chen, *J. Electroanal. Chem.*, **288,** 177 (1990).
9. M. S. Hossain, D. Tryk, and E. Yeager, *Electrochim. Acta.*, **34,** 1733 (1989).
10. D. T. Sawyer, G. Chlericato, Jr., C. T. Angells, E. J. Nannal, and T. Tsuchiya, *Anal. Chem.*, **54,** 1720 (1982).
11. K. Kinoshita, *Electrochemical Oxygen Technology*, Chap. 2, Wiley, New York (1992).
12. J. Xu, W. Huang, and R. L. McCreery, *J. Electroanal. Chem.*, **410,** 235 (1996).
13. T. Yano, D. A. Tyrk, K. Hashimoto, and A. Fujishima, *J. Electrochem. Soc.*, **145,** 1870 (1998).
14. T. Yano, E. Popa, D. A. Tyrk, K. Hashimoto, and A. Fujishima, *J. Electrochem. Soc.*, **146,** 1081 (1999).
15. I. Morcos and E. Yeager, *Electrochim. Acta.*, **15,** 953 (1970).
16. R. J. Taylor and A. A. Humffray, *J. Electroanal.Chem.*, **54,** 63 (1975).
17. Z. W. Zhang, D. A. Tyrk, and E. B. Yeager, in *Proceedings of the Workshop on the Electrochemistry of Carbon*, S. Sarangapani, J. R. Akridge, and B. Schumm, Editors, p. 158, The Electrochemical Society, Pennington, NJ (1984).
18. T. Nagaok, T. Sakai, K. Ogura, and T. Yoshino, *Anal. Chem.*, **58,** 1953 (1986).
19. J. Qayang, K. Shigehara, A. Yamada, and F. C. Anson, *Anal. Chem.*, **297,** 489 (1991).
20. J. P. Collman, N. H. Hendricks, and C. R. Leidner, Ngameni, *Inorg. Chem.*, **27,** 387 (1988).
21. J. P. Collman, P. Denisevich, Y. Konai, M. Marrocco, C. Koval, and F. C. Anson, *J. Am. Chem. Soc.*, **102,** 6027 (1980).
22. C. K. Chang, H.-Y. Liu, I. Abdalmuhdi, and F. C. Anson, *J. Am. Chem. Soc.*, **106,** 2725 (1984).
23. A. E. Martell and D. T. Sawyer, *Oxygen Complexes and Oxygen Activation by Transition Metals*, Plenum Press, New York (1988).
24. Y.-K. Choi, K.-H. Chjo, and S.-M. Park, *J. Electrochem. Soc.*, **142,** 4107 (1995).
25. J. Zagal, *Coord. Chem. Rev.*, **119,** 89 (1992).
26. D. Scherson, E. B. Yao, E. B. Yeager, J. Eldridge, M. K. Kordesh, and R. W. Hoffman, *J Phys. Chem.*, **87,** 932 (1983).
27. D. T. Fagan, I. Hu, and T. Kuwana, *Anal. Chem.*, **57,** 759 (1985).
28. J. F. Evans and T. Kuwana, *Anal. Chem.*, **51,** 358 (1979).
29. H.-H. Yang and R. L. McCreery, *Anal. Chem.*, **71,** 4081 (1999).
30. S. Ranganathan, T.-C. Kuo, and R. L. McCreery, *Anal. Chem.*, **71,** 3574 (1999).
31. E. B. Starkey, *Org. Syntheses*, **19,** 40 (1939).
32. K. E. Gubbins and R. D. Walker, *J. Electrochem. Soc.*, **112,** 469 (1965).
33. J. Chevalet, F. Roulle, D. Gerst, and J. P. Lambert, *J. Electroanal.Chem.*, **39,** 201 (1972).
34. P. Chen and R. L. McCreery, *Anal. Chem.*, **68,** 3958 (1996).
35. B. H. J. Bielski and A. O. Allen, *J. Phys. Chem.*, **81,** 1048 (1977).
36. Digisim, *Bioanalytical Systems*, Version 2.0, West Lafayette, IN (1995).
37. F. Matsumoto, K. Tokuda, T. Ahsaka, *Electroanalysis*, **8,** 648 (1996).
38. S. H. Duvall and R. L. McCreery, *Anal. Chem.*, **71,** 5494 (1999).
39. T. N. Das, T. Dhanasekaran, Z. B. Alfassi, and P. Neta, *J. Phys. Chem. A*, **102,** 280 (1998).
40. I.-F. Hu and T. Kuwana, *Anal. Chem.*, **58,** 3235 (1986).
41. M. R. Deakin, P. Kovach, K. J. Stutts, and R. M. Wightman, *Anal. Chem.*, **58,** 1474 (1986).
42. A. J. Bard and L. R. Faulkner, *Electrochemical Methods*, p. 240, Wiley, New York (1980).